Interaction of collinear transverse acoustic waves in cubic crystals

J.-Y. Duquesne and B. Perrin
LMDH, Université Pierre et Marie Curie \ CNRS (UMR 7603), Boîte 86, 4, place Jussieu, 75252 Paris Cedex 05, France
(Received 7 June 2000; published 23 January 2001)

In isotropic solids, transverse acoustic waves propagate undistorted and the interaction of collinear transverse waves is forbidden. We stress here that transverse waves behave differently in anisotropic solids and we give experimental evidence for the interaction of transverse acoustic waves propagating along the threefold axis of a cubic crystal.

DOI: 10.1103/PhysRevB.63.064303 PACS number(s): 62.65.+k, 43.25.+y

I. INTRODUCTION

It is well known that longitudinal and transverse acoustic waves exhibit different nonlinear properties in isotropic elastic solids. A longitudinal wave distorts as it propagates (second-harmonic generation) and collinear waves interact (production of harmonic waves with sum and difference frequencies). On the contrary, a transverse wave propagates without distortion and the interaction of collinear transverse waves is forbidden.[1] In anisotropic solids, the situation is somewhat different. A transverse wave can produce a second harmonic[2] and collinear transverse waves can interact. The nonlinear propagation of longitudinal waves has been observed for a long time in liquids and solids (for a review see Refs. 3–5) but, to our knowledge, very few experiments about the nonlinear propagation of transverse waves have been reported. Second-harmonic generation by transverse waves has been observed in isotropic solids, in cases where it was in principle forbidden and was then attributed to structural defects.[6,7] Second-harmonic generation by transverse waves has also been observed in ac-cut quartz but the nonlinear coupling parameter was found to depend strongly on the sample so that impurities or dislocation effects were suspected.[8] Recently, we observed second-harmonic generation by transverse waves in an icosahedral quasicrystal.[9] In the present paper, we report experiments performed in silicon which show evidence for the intrinsic nonlinear behavior of transverse waves propagating in a cubic crystal. We observed the production of sum frequency waves when two transverse acoustic waves with different frequency propagate simultaneously along a threefold axis. This behavior is in good agreement with our theoretical analysis and results from the intrinsic nonlinearities of the solid.

II. THEORY

Let us consider the nonlinear propagation of an acoustic plane wave along a given direction. The equations of motion are conveniently expressed in a set of rectangular Cartesian coordinate axes which includes the propagation direction. Let us call *xyz* such a coordinate set, where x is the propagation direction. The equations of motion are then

$$\rho u_{1,tt} - C'_{11}u_{1,xx} - C'_{16}u_{2,xx} - C'_{15}u_{3,xx} = f(u_{1,x}, u_{2,x}, u_{3,x}), \tag{1}$$

$$\rho u_{2,tt} - C'_{16}u_{1,xx} - C'_{66}u_{2,xx} - C'_{56}u_{3,xx} = g(u_{1,x}, u_{2,x}, u_{3,x}), \tag{2}$$

$$\rho u_{3,tt} - C'_{15}u_{1,xx} - C'_{56}u_{2,xx} - C'_{55}u_{3,xx} = h(u_{1,x}, u_{2,x}, u_{3,x}), \tag{3}$$

where u_i are the displacement components, ρ is the mass density and C'_{ij} are the second-order elastic constants, expressed in the *xyz* coordinate axes. The right-hand terms f, g, and h arise from the intrinsic nonlinear properties of the solid and depend on the higher-order elastic constants. These source terms can, under due circumstances, induce a nonlinear behavior of the acoustic waves: the interaction of waves and production of second-harmonic waves. They are small and Appendix A gives their expressions in a second-order approximation. Approximate solutions of Eqs. (1)–(3) can be obtained by a perturbation method.[10,11] The displacement field is written $u = u^{[I]} + u^{[II]}$, where $u^{[I]}$ is the primary displacement field (i.e., the solution when the nonlinear source terms are neglected), and where $u^{[II]}$ is a small correction. In Eqs. (1)–(3), $u^{[II]}$ is then substituted to u on the left-hand side and $u^{[I]}$ is substituted to u on the right-hand side. In this paper, we only consider primary transverse waves: $u_1^{[I]} = 0$. In the following, the source terms will then be $f(0, u_{2,x}^{[I]}, u_{3,x}^{[I]})$, $g(0, u_{2,x}^{[I]}, u_{3,x}^{[I]})$, and $h(0, u_{2,x}^{[I]}, u_{3,x}^{[I]})$. In isotropic solids, the g and h source terms vanish because the elastic constants C'_{15}, C'_{16}, C'_{56}, C'_{156}, C'_{555}, C'_{556}, C'_{566} and C'_{666} are equal to zero. Then, a primary transverse wave propagates without distortion and collinear transverse waves do not interact. A harmonic longitudinal field $u_1^{[II]}$ is produced because the f source term does not vanish. However, its amplitude does not grow but oscillates along the propagation direction because of the phase mismatch between longitudinal and transverse waves.[1] We stress here that the nonlinear behavior of transverse waves may be different in an anisotropic solid since the g and h source terms may be nonzero. In those cases, the possibility for the production of harmonic transverse fields must be considered.

To be specific, let us consider the nonlinear propagation of transverse acoustic waves along the threefold axis [111] of a cubic crystal. We use the following rectangular Cartesian coordinate axes: $x = [111]$, $y = [11\bar{2}]$, $z = [\bar{1}10]$. The equations of motion are then (see Appendixes A and B)

$$\rho u^{[II]}_{1,tt} - C'_{11} u^{[II]}_{1,xx} = \frac{\partial}{\partial x}\left\{ \frac{1}{2}(C'_{11} + C'_{155})[(u^{[I]}_{2,x})^2 + (u^{[I]}_{3,x})^2] \right\}, \tag{4}$$

$$\rho u^{[II]}_{2,tt} - C'_{55} u^{[II]}_{2,xx} = \frac{\partial}{\partial x}\left\{ \frac{1}{2} C'_{666}[(u^{[I]}_{2,x})^2 - (u^{[I]}_{3,x})^2] - C'_{555} u^{[I]}_{2,x} u^{[I]}_{3,x} \right\}, \tag{5}$$

$$\rho u^{[II]}_{3,tt} - C'_{55} u^{[II]}_{3,xx} = \frac{\partial}{\partial x}\left\{ -\frac{1}{2} C'_{555}[(u^{[I]}_{2,x})^2 - (u^{[I]}_{3,x})^2] - C'_{666} u^{[I]}_{2,x} u^{[I]}_{3,x} \right\}. \tag{6}$$

The primary transverse waves are degenerate, with polarizations in the *yz* plane, and the source terms in Eqs. (5) and (6) do not vanish. Then a transverse wave will distort as it propagates and collinear primary transverse waves will interact. Let us consider two primary collinear transverse waves, propagating along [111], in the same direction, with circular frequency ω_1 and ω_2 and polarization angles ϕ_1 and ϕ_2 in the *yz* plane. The primary acoustic field is

$$\begin{pmatrix} u^{[I]}_1 \\ u^{[I]}_2 \\ u^{[I]}_3 \end{pmatrix} = \begin{pmatrix} 0 \\ a\cos\phi_1 \\ a\sin\phi_1 \end{pmatrix} \cos\Omega_1 + \begin{pmatrix} 0 \\ b\cos\phi_2 \\ b\sin\phi_2 \end{pmatrix} \cos\Omega_2, \tag{7}$$

where

$$\Omega_i = \omega_i t - k_i x + \theta_i, \tag{8}$$

$$k_i^2 C'_{55} = \rho\omega_i^2, \tag{9}$$

$$k_1 k_2 > 0. \tag{10}$$

The source terms will produce a harmonic transverse field with $2\omega_1$, $2\omega_2$, $(\omega_1+\omega_2)$, and $(\omega_1-\omega_2)$ components. Let us only consider the $\omega_1+\epsilon\omega_2$ components ($\epsilon=\pm1$). We get

$$u^{[II]}_2 = \epsilon A x \cos(\Phi - \phi_1 - \phi_2)\cos(\Omega_1 + \epsilon\Omega_2), \tag{11}$$

$$u^{[II]}_3 = \epsilon A x \sin(\Phi - \phi_1 - \phi_2)\cos(\Omega_1 + \epsilon\Omega_2), \tag{12}$$

where

$$A = -\frac{abk_1k_2}{4}\frac{\sqrt{C'^2_{555} + C'^2_{666}}}{C'_{55}}, \tag{13}$$

$$\sin\Phi = \frac{C'_{555}}{\sqrt{C'^2_{555} + C'^2_{666}}}, \tag{14}$$

$$\cos\Phi = \frac{-C'_{666}}{\sqrt{C'^2_{555} + C'^2_{666}}}. \tag{15}$$

TABLE I. Polarization of the harmonic transverse waves versus selected polarizations of the primary transverse waves for cubic crystals in the $m3m$, $\bar{4}3m$, and 432 classes. All waves propagate along the [111] direction.

	Primary wave (ω_1)	Primary wave (ω_2)	Harmonic wave ($\omega_1+\epsilon\omega_2$)
Polarization	$[11\bar{2}]$	$[11\bar{2}]$	$[11\bar{2}]$
Polarization	$[11\bar{2}]$	$[\bar{1}10]$	$[\bar{1}10]$
Polarization	$[\bar{1}10]$	$[\bar{1}10]$	$[11\bar{2}]$

Then primary transverse waves propagating in a cubic crystal along a threefold axis [111] with polarization angles ϕ_1 and ϕ_2 do interact and produce harmonic transverse waves which grow linearly with the propagation distance *x*. The polarization angle ψ of the harmonic waves in the *yz* plane is given by the relation

$$\psi = \Phi - \phi_1 - \phi_2. \tag{16}$$

Of course, this law is consistent with the threefold symmetry around [111]. For cubic crystals in the $m3m$, $\bar{4}3m$, and 432 classes, the expressions further simplify since $C'_{555} = 0$ and the relation (16) becomes independent of the elastic constants

$$\psi = -(\phi_1 + \phi_2). \tag{17}$$

Table I gives the polarization of the harmonic transverse waves versus selected polarizations of the primary transverse waves for cubic crystals in the $m3m$, $\bar{4}3m$, and 432 classes. In the same way, for second-harmonic generation, we get ($\psi = -2\phi$), where ϕ is the primary wave polarization angle. Then, the angle between the polarizations of the primary wave and its second harmonic can exhibit a range of values between 0 and π. In particular, a primary wave polarized parallel to [110] and its second harmonic will have perpendicular polarizations, whereas a primary wave polarized normal to [110] and its second harmonic will have parallel polarizations.

Using the same method, it is easy to study the nonlinear propagation of transverse waves in a cubic crystal along a [100] or along a [110] axis (see Appendixes A and B for the relevant elastic constants). Transverse waves propagating along a [100] axis do not interact and do not distort as they propagate because the source terms vanish. The behavior of transverse waves propagating along a [110] axis depends on the cubic class. In the $m3m$, $\bar{4}3m$, and 432 classes, they do not interact and do not distort as they propagate because the source terms vanish. In the less symmetrical $m3$ or 23 classes, the source terms do not vanish. However, waves polarized along $[\bar{1}10]$ or [001] have different velocities so that phase mismatching must be considered. We find that only transverse waves polarized along $[\bar{1}10]$ do interact and distort as they propagate (the harmonic field is polarized along $[\bar{1}10]$).

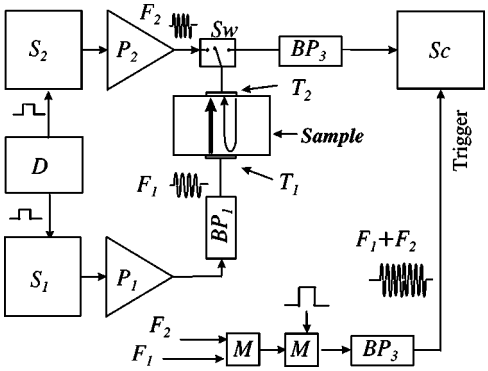

FIG. 1. Sketch of the setup. The transducers T_1 and T_2 are driven by two pulsed high-frequency sources. The delay generator D synchronizes the emission of the acoustic pulses with frequency F_1 and F_2. An electronic switch Sw selects the operation mode of T_2 (transmitter or receiver). S_1,S_2 are high-frequency synthetizers (pulse modulated). P_1,P_2 are power amplifiers. BP_3 and BP_1 are band-pass filters at 160 and 45 MHz, respectively. Sc is a digital scope. M is a mixer. $F_1=45$ MHz,$F_2=117$ MHz.

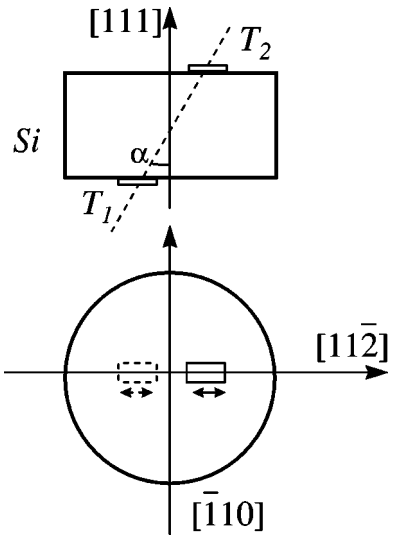

FIG. 2. Position and orientation of the transducers T_1 and T_2 used in the study of Si[111]. The double arrows show the polarization of the transducers (parallel to $[11\bar{2}]$). α is the angular deviation of the power flow from the [111] axis. In Si: $\alpha=13°$.

III. EXPERIMENTS

We have studied the interaction of collinear transverse waves in silicon ($m3m$ cubic point group). The samples are single crystals with a low impurity content (room-temperature resistivity $>100\ \Omega$ cm). Two samples are used in order to compare the interaction of collinear transverse waves propagating along a threefold axis [111] and along a fourfold axis [100]. On both samples, two oriented faces are polished, flat and parallel: respectively, two (111) and two (100) faces. Both samples are cylinders with a length d equal to 10.0 mm and a diameter equal to 18 mm. The transverse waves transducers are $LiNbO_3$ plates (163° rotated, Y cut). Two transducers T_1 and T_2 are glued on both faces of a given sample with salol. Their polarizations are well controlled. The size of the electrodes is 2 mm$\times$3 mm. The same set of transducers is used for both samples.

Figure 1 is a sketch of the setup used to detect the possible transverse harmonic waves. The T_1 and T_2 transducers are driven by separate high-frequency pulsed sources at $F_1=45$ MHz and $F_2=117$ MHz, respectively. The P_1 and P_2 amplifiers are 50-Ω broadband power amplifiers. They deliver 7 and 1 W, respectively (on a 50 Ω load). T_2 is also able to detect waves at $(F_1+F_2)=162$ MHz. Then, T_2 is both the source for the F_2 primary wave and the receiver for possible (F_1+F_2) harmonic waves. An electronic switch Sw selects the mode of operation of T_2. The excitation pulses are delayed with respect to one another to ensure the simultaneous propagation of the F_1 and F_2 acoustic pulses. For that purpose, the F_1 acoustic pulse is emitted when the F_2 acoustic pulse arrives at T_1. Then, the emitted F_1 acoustic pulse and the reflected F_2 acoustic pulse propagate simultaneously from one face to the other. The received signal is filtered and recorded by a digital scope, triggered by synchronous (F_1+F_2) electric pulses. Averaging is performed to improve the signal-to-noise ratio.

In Si[100], the polarizations of the transducers (and then of the acoustic waves) are set parallel to an arbitrary direction and the transducers are face to face. In the case of Si[111], the internal conical refraction must be considered. It is well known that the power flow of transverse waves propagating along [111] is deflected from [111]. The Poynting vector rotates about a cone when the polarization is rotated in the plane normal to [111].[12] The semiangle of this cone is 13° in Si. Then, because of the finite size of the transducers, acoustic beams propagating in the same direction along [111] but with different polarizations will only overlap in a restricted volume. In such a case, the expected interaction of the waves will occur only in this restricted volume and the benefit from cumulative effects will be lost. Then, in our experiment, it is desirable that the primary waves have the same polarization angle: $\phi_1\equiv\phi_2\ [\pi]$. Let us call ϕ this common polarization. An additional restriction arises from the polarization angle -2ϕ of the expected harmonic wave. To benefit from a cumulative effect, the power flow of this harmonic must be in the same direction as the power flow of the fundamental waves. Then the harmonic and the fundamental waves should have the same polarization angle: $\phi\equiv-2\phi[\pi]$. Optimal conditions for the experiment are then obtained for ϕ equal to $-\pi/3$, 0, or $+\pi/3$. Indeed those conditions are equivalent because of the threefold symmetry around [111]. The present experiments in Si[111] were performed with $\phi=0$: the polarizations of the transducers are set parallel to $[11\bar{2}]$, i.e., normal to a twofold axis. Moreover, the transducers are shifted with respect to one another along $[11\bar{2}]$ to take into account the power flow deviation. Figure 2 is a sketch of the configuration.

It is important in the experiments that the acoustic powers of the fundamental waves are as closed as possible in both samples. We compared then the electromechanical conversion factors K of the transducers successively glued on Si[111] and Si[100]. For that purpose, we measured the magnitude of the first echo in the reflexion mode, for each sample and each transducer (in that case, the transducer op-

TABLE II. Ratio of the electromechanical coupling factor K (one conversion) of the transducers T_1 and T_2 when glued successively on Si[111] and Si[100].

Transducer	T_1	T_2	T_2
Frequency	45 MHz	117 MHz	162 MHz
K[111]/K[100]	2.4 dB	-1 dB	-2.7 dB

erates either as a transmitter or as a receiver). The ratio of the conversion factors was then deduced. We observed that the conversion factor of a given transducer was nearly constant, within a few dB, in the experiments on both samples. Table II gives our results.

Figure 3 displays the signals which were observed successively in Si[111] and Si[100]. Pulses were observed at $(F_1+F_2)=162$ MHz. They are large in Si[111] and, on the contrary, small in Si[100]. The amplitude ratio is 26 dB (first pulses). We swapped several times the Si[111] and Si[100] samples. Qualitatively, the same observation was performed. Figure 4 displays, in Si[111], $\log_{10}E$ versus $\log_{10}A_1A_2$, where E is the amplitude of the first pulse at (F_1+F_2), and where A_1 and A_2 are the amplitudes of the first pulses at F_1 and F_2, respectively. We observe that E is proportional to the product A_1A_2.

Clearly, the (F_1+F_2) pulses result from some nonlinear processes. The comparison of the results in both samples shows that the nonlinear processes are more efficient when using the Si[111] sample than when using the Si[100] sample. Since the setups are otherwise identical, we suggest that the pulses observed when using Si[111] are mainly due to a nonlinear process located inside the sample. Our results are in good agreement with the theoretical analysis: transverse waves propagating along [111] interact and produce sum frequency waves, whereas transverse waves propagating along [100] do not. The large difference in the pulse amplitudes in Si[111] and Si[100] cannot be accounted for by

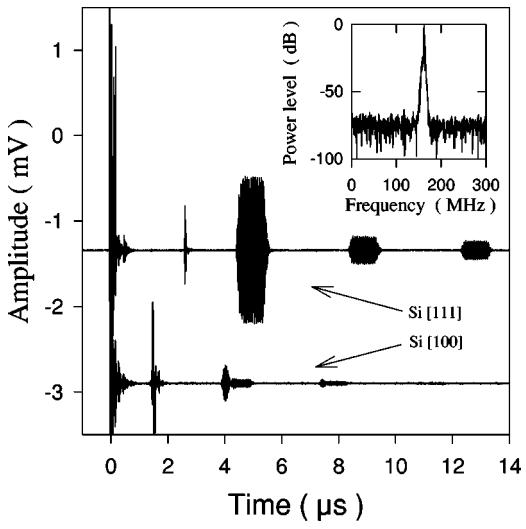

FIG. 3. Harmonic signals observed in Si[111] and Si[100]. The inset is the power spectrum of the first pulse in Si[111] (between 4 and 6 μs).

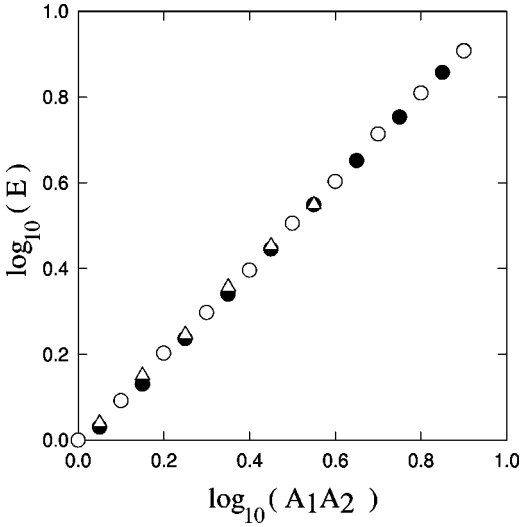

FIG. 4. $\log_{10}E$ versus $\log_{10}A_1A_2$ in Si[111]. E, A_1, and A_2 are the amplitudes of the first harmonic pulse (at F_1+F_2) and of the first fundamental pulses (at F_1 and F_2), respectively. Different arbitrary units are used for E and A_1A_2. Black dots: A_2 is kept constant and A_1 varies. White dots: A_1 is kept constant and A_2 varies. White triangles: A_1 is kept constant (previous A_1 level minus 7 dB) and A_2 varies.

different power levels of the primary acoustic waves in both samples since the conversion factors of the transducers are very closed when glued successively on both samples (Table II). For the same reason, it cannot be accounted for by different sensitivities of the receiver. No interaction is expected in Si[100] and the small pulses that are observed there are most likely due to a nonlinear characteristic of the transducers. We have checked that the order of magnitude of the first (F_1+F_2) pulse in Si[111] was in agreement with the value derived from Eq. (13) (where Φ and $\phi_1+\phi_2$ vanish), using estimates of the electromechanical conversion factors and of the electrical power inputs, as well as published values of the elastic constants.[13] Then, we believe that our experimental results show that the intrinsic nonlinearities of silicon induce an interaction of collinear transverse acoustic waves propagating along [111].

IV. CONCLUSION

We have analyzed in detail the nonlinear propagation of transverse acoustic waves along symmetry axes of cubic crystals. The equations of motion show that transverse waves propagating along a threefold axis distort as they propagate and interact. This behavior is qualitatively different from what happens in isotropic solids. We have performed experiments in silicon in order to investigate the interaction of transverse waves. We observed that two transverse waves with frequency F_1 and F_2, propagating simultaneously along a threefold axis and polarized normal to a twofold axis, produce a transverse harmonic wave with frequency (F_1+F_2). This shows evidence that the intrinsic nonlinearities of an anisotropic solid can induce an interaction of collinear transverse acoustic waves.

ACKNOWLEDGMENTS

It is a pleasure to thank Dr. A. Levelut for useful discussions.

APPENDIX A

Equations (A1)–(A3) give the expressions of the source terms in Eqs. (1)–(3) in a second-order approximation. The elastic constants are expressed in arbitrary Cartesian coordinates axes *xyz*. C'_{ij} are the second-order elastic constants. C'_{ijk} are the Brugger third-order elastic constants.

$$f(\alpha,\beta,\gamma)=\frac{\partial}{\partial x}\left\{\begin{array}{l}\frac{1}{2}(3C'_{11}+C'_{111})\alpha^2+\frac{1}{2}(C'_{11}+C'_{166})\beta^2+\frac{1}{2}(C'_{11}+C'_{155})\gamma^2\\ +(C'_{16}+C'_{116})\alpha\beta+(C'_{15}+C'_{115})\alpha\gamma+C'_{156}\beta\gamma\end{array}\right\}, \tag{A1}$$

$$g(\alpha,\beta,\gamma)=\frac{\partial}{\partial x}\left\{\begin{array}{l}\frac{1}{2}(C'_{16}+C'_{116})\alpha^2+\frac{1}{2}(3C'_{16}+C'_{666})\beta^2+\frac{1}{2}(C'_{16}+C'_{556})\gamma^2\\ +(C'_{11}+C'_{166})\alpha\beta+C'_{156}\alpha\gamma+(C'_{15}+C'_{566})\beta\gamma\end{array}\right\}, \tag{A2}$$

$$h(\alpha,\beta,\gamma)=\frac{\partial}{\partial x}\left\{\begin{array}{l}\frac{1}{2}(C'_{15}+C'_{115})\alpha^2+\frac{1}{2}(C'_{15}+C'_{566})\beta^2+\frac{1}{2}(3C'_{15}+C'_{555})\gamma^2\\ +C'_{156}\alpha\beta+(C'_{11}+C'_{155})\alpha\gamma+(C'_{16}+C'_{556})\beta\gamma\end{array}\right\}. \tag{A3}$$

APPENDIX B

Tables III, IV, and V give the expressions of the second-order elastic constants and the Brugger third-order elastic constants, in the cubic system, in three different Cartesian coordinates axes:

Coordinates axes No. 1: [100],[010],[001] (standard coordinates axes).

Coordinates axes No. 2: [110],[$\bar{1}$10],[001]

Coordinates axes No. 3: [111],[11$\bar{2}$], [$\bar{1}$10]

These three sets of coordinate axes are useful to study the acoustic propagation in the [100], [110], and [111] directions, respectively. Only the constants relevant to Eqs. (1)–(3) are given. The elastic constants in the standard Cartesian coordinate axes are labeled C_{ij} and C_{ijk}. Those in the arbitrary Cartesian coordinate axes are labeled C'_{ij} and C'_{ijk}. Table III gives the second-order elastic constants (valid for all cubic classes). Tables IV and V give the third-order elastic constants in the low-symmetry cubic classes ($m3$ and 23) and high-symmetry cubic classes ($m3m$, $\bar{4}3m$, or 432), respectively. Table V is derived from Table IV with the additional properties: ($C_{112}=C_{113}$) and ($C_{155}=C_{166}$).

TABLE III. Second-order elastic constants C'_{ij} in various coordinates systems versus second-order elastic constants C_{ij} in the standard coordinate axes. Cubic system.

	Coordinate axes No. 1	Coordinate axes No. 2	Coordinate axes No. 3
C'_{11}	C_{11}	$\frac{1}{2}(C_{11}+C_{12}+2C_{44})$	$\frac{1}{3}(C_{11}+2C_{12}+4C_{44})$
C'_{15}	0	0	0
C'_{16}	0	0	0
C'_{55}	C_{44}	C_{44}	$\frac{1}{3}(C_{11}-C_{12}+C_{44})$
C'_{56}	0	0	0
C'_{66}	C_{44}	$\frac{1}{2}(C_{11}-C_{12})$	$\frac{1}{3}(C_{11}-C_{12}+C_{44})$

TABLE IV. $m3$ and 23 cubic classes. Third-order Brugger elastic constants C'_{ijk} in various coordinates systems versus third-order Brugger elastic constants C_{ijk} in the standard coordinate axes.

	Coordinate axes No. 1	Coordinate axes No. 2	Coordinate axes No. 3
C'_{111}	C_{111}	$\frac{1}{8}(2C_{111}+3C_{112}+3C_{113}+12C_{155}+12C_{166})$	$\frac{1}{9}(C_{111}+3C_{112}+3C_{113}+2C_{123}+12C_{144}+12C_{155}+12C_{166}+16C_{456})$
C'_{115}	0	0	0
C'_{116}	0	$\frac{1}{8}(-C_{112}+C_{113}+4C_{155}-4C_{166})$	0
C'_{155}	C_{155}	$\frac{1}{4}(2C_{144}+C_{155}+C_{166}+4C_{456})$	$\frac{1}{9}(C_{111}-C_{123}-3C_{144}+3C_{155}+3C_{166}-2C_{456})$
C'_{156}	0	0	0
C'_{166}	C_{166}	$\frac{1}{8}(2C_{111}-C_{112}-C_{113})$	C'_{155}
C'_{555}	0	0	$\frac{\sqrt{6}}{12}(C_{112}-C_{113}-C_{155}+C_{166})$
C'_{556}	0	$\frac{1}{4}(-C_{155}+C_{166})$	$\frac{\sqrt{2}}{36}(2C_{111}-3C_{112}-3C_{113}+4C_{123}+6C_{144}-3C_{155}-3C_{166}-4C_{456})$
C'_{566}	0	0	$-C'_{555}$
C'_{666}	0	$\frac{3}{8}(C_{112}-C_{113})$	$-C'_{556}$

TABLE V. $m3m$, $\bar{4}3m$, and 432 cubic classes. Third-order Brugger elastic constants C'_{ijk} in various coordinates systems versus third-order Brugger elastic constants C_{ijk} in the standard coordinate axes.

	Coordinate axes No. 1	Coordinate axes No. 2	Coordinate axes No. 3
C'_{111}	C_{111}	$\frac{1}{4}(C_{111}+3C_{112}+12C_{155})$	$\frac{1}{9}(C_{111}+6C_{112}+2C_{123}+12C_{144}+24C_{155}+16C_{456})$
C'_{115}	0	0	0
C'_{116}	0	0	0
C'_{155}	C_{155}	$\frac{1}{2}(C_{144}+C_{155}+2C_{456})$	$\frac{1}{9}(C_{111}-C_{123}-3C_{144}+6C_{155}-2C_{456})$
C'_{156}	0	0	0
C'_{166}	C_{155}	$\frac{1}{4}(C_{111}-C_{112})$	C'_{155}
C'_{555}	0	0	0
C'_{556}	0	0	$\frac{\sqrt{2}}{18}(C_{111}-3C_{112}+2C_{123}+3C_{144}-3C_{155}-2C_{456})$
C'_{566}	0	0	0
C'_{666}	0	0	$-C'_{556}$

[1] Z.A. Gol'dberg, Sov. Phys. Acoust. **6**, 306 (1961).
[2] A.C. Holt and J. Ford, J. Appl. Phys. **38**, 42 (1967).
[3] A. N. Norris, in *Nonlinear Acoustics*, edited by M. F. Hamilton and D. T. Blackstock (Academic Press, San Diego, 1998), p. 263.
[4] R. T. Beyer, in *Nonlinear Acoustics* (Ref. 3), p. 25.
[5] M. A. Breazeale and J. Philip, in *Physical Acoustics*, edited by W. P. Mason and R. N. Thurston (Academic Press, New York, 1984), Vol. XVII, Chap. I.
[6] A.A. Gedroits, L.K. Zarembo, and V.A. Krasil'nikov, Dokl. Akad. Nauk (SSSR) **150**, 515 (1963) [Sov. Phys. Dokl. **8**, 478 (1963)].
[7] L.K. Zarembo and V.A. Krasil'nikov, Usp. Fiz. Nauk **102**, 549 (1970) [Sov. Phys. Usp. **13**, 778 (1971)].
[8] P.H. Carr, Phys. Rev. **169**, 718 (1968).
[9] J.-Y. Duquesne and B. Perrin, Phys. Rev. Lett. **85**, 4301 (2000).
[10] G.L. Jones and D.R. Kobett, J. Acoust. Soc. Am. **35**, 5 (1963).
[11] R. Truell, C. Elbaum, and B. B. Chick, *Ultrasonic Methods in Solid State Physics* (Academic Press, New York, 1969).
[12] B. A. Auld, *Acoustic Fields and Waves in Solids* (Wiley-Interscience, New York, 1973), Vol. II.
[13] J.J. Hall, Phys. Rev. **161**, 756 (1967).